JOURNAL OF CATALYSIS 11, 46–53 (1968)

# Studies on Pore Systems in Catalysts

## XV. The Influence of the Geometrical Factor on the $t$ Curve Measured on Aerosil

J. H. DE BOER, B. G. LINSEN,* J. C. P. BROEKHOFF, AND TH. J. OSINGA*

*From the Department of Chemical Technology, Technological University of Delft, The Netherlands*

Received February 6, 1968

In a previous article of this series it was shown that the $t$ curve measured on Aerosil greatly deviates from the common $t$ curve. In this article we shall treat this phenomenon in more detail. From the nitrogen-sorption isotherms, measured on four different aerosils, the $t$ curves are calculated. It is shown that the magnitude of the deviations from the common $t$ curve depends on the particle size of Aerosil. By calculations, based on geometrical and thermodynamic considerations, theoretical $t$ values are obtained in perfect agreement with the experimental ones.

### I. INTRODUCTION

In Part VI of this series (*1*) the adsorption of nitrogen at −196°C on various well-defined samples ($Al_2O_3$, $TiO_2$, $ZrO_2$, MgO, Ni-antigorite, $SiO_2$, and three graphitized carbon blacks) was discussed. The statistical thickness $t$ of the layer of nitrogen adsorbed was measured as a function of the relative pressure and compared with the $t$ curve given in Article I of this series (*2*). This statistical thickness was calculated according to the equation

$$t = 3.54(V_a/V_m)\ \text{Å} \qquad (1)$$

where $V_a$ is the adsorbed volume of the adsorbate in ml gas STP/g adsorbent and $V_m$ is the volume of gas required to cover the whole surface area of the solid substance unimolecularly, also expressed in ml STP/g adsorbent, calculated by the BET method (*3*). It was shown that the $t$ curves measured on $Al_2O_3$, $TiO_2$, MgO, $ZrO_2$, $BaSO_4$, and nickel antigorite are practically identical. An appreciable influence of the nature of the surface on the thickness of the adsorbed layer was not observed.

Using the $V_m$ value calculated with the BET equation in Eq. (1) the $t$ values of the graphitized carbon blacks do not correspond with the common $t$ curve. However, plotting $V_a$ as a function of the thickness $t$ measured on alumina, gives a straight line through the origin and shows that only the points corresponding to lower pressures deviate from this straight line. This phenomenon is fully discussed in the Articles VI (*1*) and and VIII (*4*) of this series.

In the case of $SiO_2$ (Aerosil Degussa), the $t$ values calculated for relative pressures $< 0.15$ are nearly identical with those of alumina. For relative pressures $> 0.15$, the thickness $t$ calculated for $SiO_2$ greatly deviates from the values measured with alumina. This phenomenon is also clearly shown by plotting $V_a$ as a function of $t$. In that case below a $t$ value of 4 Å a straight line through the origin can be drawn. Above a $t$ value of 4 Å the curve bends downwards.

A simple explanation would be that the particles of Aerosil contain narrow pores. This explanation would be in agreement with the work of Geus and Kiel (*5*). The latter authors state that the particles of Aerosil consist of small nonporous particles of about 15 Å, between which narrow pores may be present.

Another explanation would be the open

---

* Present address: Unilever Research Laboratory, Vlaardingen, The Netherlands.

structure of the arrangement of the surface atoms of nonporous silica gel particles (*6*). In that case too high a value may be calculated for the capacity of the monomolecular layer ($V_m$). As a result of it the calculated value for the thickness is too small and deviations in the $t$ curve may also occur.

A third explanation is based on geometric considerations. The particles of Aerosil are built up of very small nonporous spherical particles. The surface available for adsorption is not constant during adsorption, but a function of the thickness $t$ and of the average number of particles touching each particle, which we shall indicate by the coordination number. As a result of this texture, using Eq. (1) a formal thickness ($t_f$) (Ref. *12*) of the adsorbed layer will be found and not the actual one ($t$).

The last explanation is based on the general phenomenon that the curvature of a surface has an influence on the adsorption. The thermodynamic treatment of this phenomenon has been given in Article IX (*7*) of this series, in which is shown that the thickness of the adsorbed layer of nitrogen on a curved surface is different from that on a flat surface at the same pressure.

In this article we will restrict ourselves to the last two explanations, which are considered to be the most plausible. We will show quantitatively for four different Aerosils *ex* Degussa the influence of the curvature of the surface, being a function of the size of the particles, together with the influence of the coordination number on the $t$ values obtained with Eq. (1).

## II. Experimental and Results

The nitrogen adsorption isotherms of four commercial Aerosil samples *ex* Degussa (Germany) were measured. The adsorption measurements were carried out with the micro-BET apparatus as described in Part I (*2*) of this series. The BET surface area and the radii of the elementary particles ($r_p$) of these samples are given in Table 1. The radii were calculated by means of the equation

$$r_p = (3V_{\text{spec}}/S_{\text{BET}}) \times 10^4\ \text{Å} \qquad (2)$$

in which $V_{\text{spec}}$ is the specific volume in ml/g of silica.

From the nitrogen adsorption isotherms the thickness of the adsorbed layer was calculated by means of Eq. (1). The results are given in the Figs. 1–4. For comparative purposes these four curves are drawn again in Fig. 5 together with the common $t$ curve as given in Articles I (*2*) and VI (*1*) of this series.

## III. Discussion

### 1. *The Influence of the Geometry on the t Curve*

Figure 5 clearly shows that the curves measured for Aerosil greatly deviate from

TABLE 1

Comparison between Measured and Calculated Thickness of the Adsorbed Layer Not Taking into Account the Curvature of the Surface

| | | I<br>$r = 80$ Å<br>$\theta = 153°$<br>$S_{\text{BET}} = 162$ m²/g | | II<br>$r = 46$ Å<br>$\theta = 145°$<br>$S_{\text{BET}} = 281$ m²/g | | III<br>$r = 39$ Å<br>$\theta = 142°$<br>$S_{\text{BET}} = 333$ m²/g | | IV<br>$r = 33$ Å<br>$\theta = 139°$<br>$S_{\text{BET}} = 394$ m²/g | |
|---|---|---|---|---|---|---|---|---|---|
| $p/p_0$ | Common $t$ | $t_f$ measured | $t_f$ calc. | $t_f$ measured | $t_f$ calc. | $t_f$ measured | $t_f$ calc. | $t_f$ measured | $t_f$ calc. |
| 0.032 | 3 | 2.96 | 2.96 | 2.90 | 2.95 | 2.98 | 2.95 | 2.95 | 2.95 |
| 0.146 | 4 | 4.01 | 3.94 | 3.99 | 3.90 | 4.00 | 3.89 | 3.95 | 3.87 |
| 0.300 | 5 | 4.91 | 4.89 | 4.90 | 4.81 | 4.83 | 4.78 | 4.72 | 4.73 |
| 0.440 | 6 | 5.72 | 5.83 | 5.75 | 5.68 | 5.62 | 5.61 | 5.42 | 5.52 |
| 0.562 | 7 | 6.58 | 6.74 | 6.55 | 6.51 | 6.38 | 6.39 | 6.08 | 6.24 |
| 0.660 | 8 | 7.60 | 7.63 | 7.40 | 7.28 | 7.23 | 7.11 | 6.78 | 6.89 |
| 0.725 | 9 | 8.45 | 8.50 | 8.26 | 8.01 | 7.97 | 7.77 | 7.42 | 7.46 |
| 0.778 | 10 | 9.34 | 9.34 | 9.20 | 8.69 | 8.68 | 8.37 | 8.08 | 7.94 |
| 0.818 | 11 | 10.10 | 10.16 | 10.00 | 9.32 | 9.35 | 8.89 | 8.76 | 8.33 |

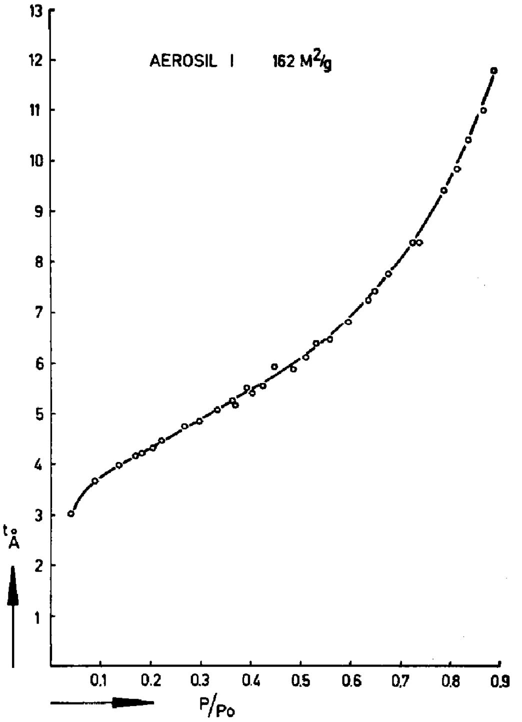

Fig. 1. Formal thickness as a function of the relative pressure, Aerosil I.

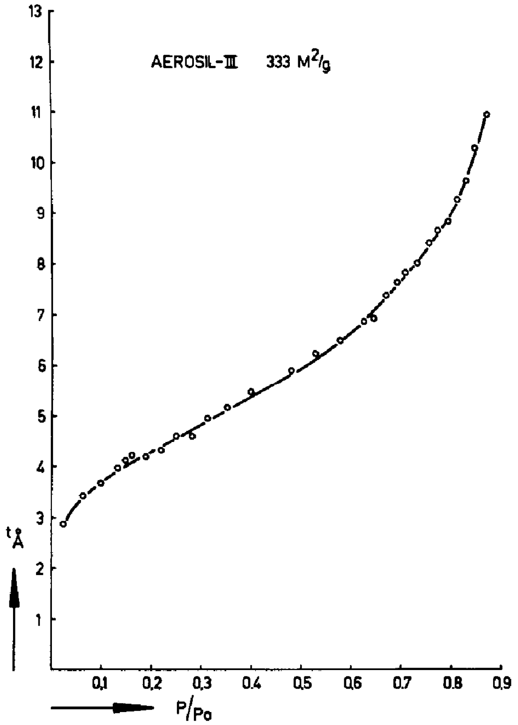

Fig. 3. Formal thickness as a function of the relative pressure, Aerosil III.

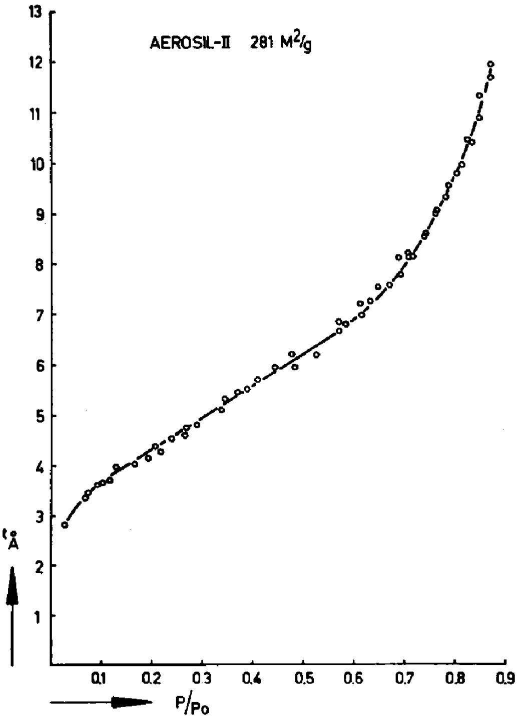

Fig. 2. Formal thickness as a function of the relative pressure, Aerosil II.

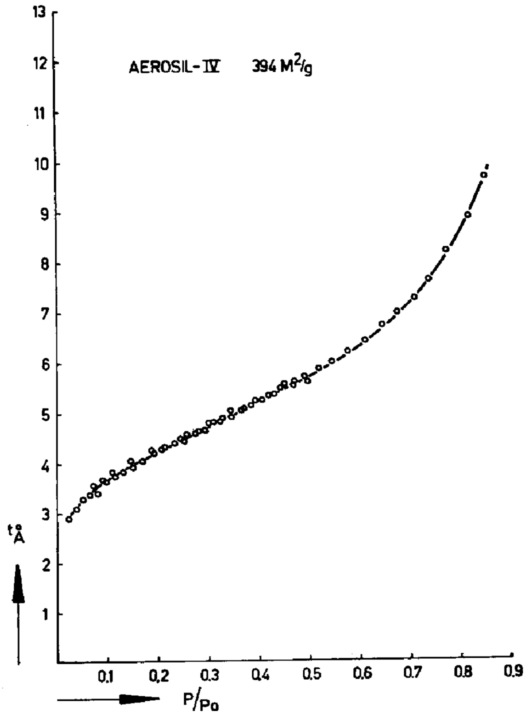

Fig. 4. Formal thickness as a function of the relative pressure, Aerosil IV.

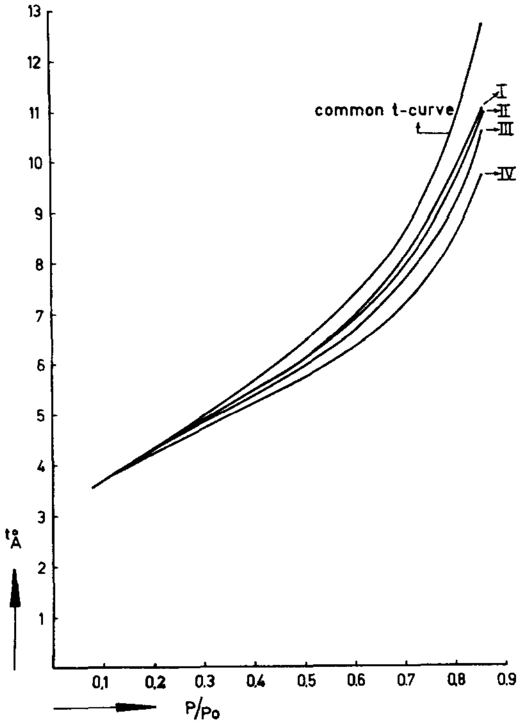

FIG. 5. Comparison between the common $t$ curve and the curves measured on the Aerosil samples.

the common $t$ curve. This deviation increases with decreasing particle size. The common curve is derived from adsorption isotherms measured on samples with flat surfaces and in which no capillary condensation takes place. Aerosil, however, is built up of very small elementary spherical particles, as a result of which it may be expected that deviations occur. If only one small particle is available for adsorption, the surface area on which successive layers are adsorbed, increases. In that case the $t$ curve obtained by means of Eq. (1) will be situated above the common $t$ curve. If, however, each elementary particle is in contact with several others, narrow edges are formed between each two neighboring particles. During adsorption these edges are filled up with nitrogen, as result of which the surface area available for adsorption decreases constantly. In this case the $t$ curve obtained by means of Eq. (1) will be situated below the common $t$ curve. If it is assumed that the elementary particles of the Aerosil preparations are perfect spheres of uniform size and have a completely smooth surface — an electron micrograph and the method of preparation (*8*) make this acceptable — it is possible to calculate quantitatively the deviating $t_f$ curves, using the radii of the particles given in Table 1 and assuming a certain coordination number found by trial and error. The geometrical pattern obtained for spherical elementary particles is given in Fig. 6.

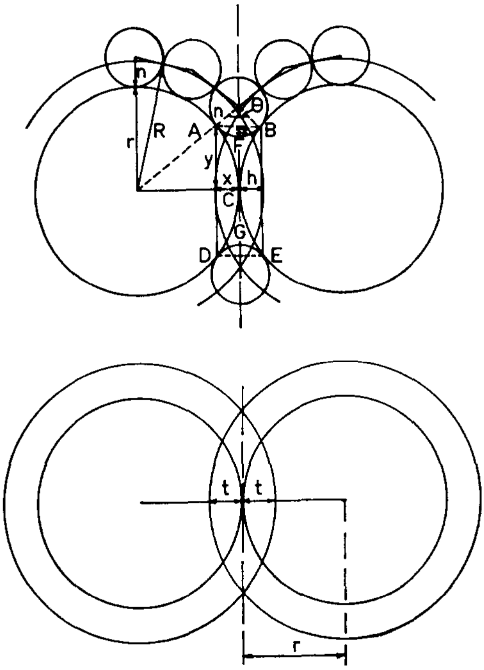

FIG. 6. Geometrical pattern of the adsorbed layer on spherical particles.

In this figure, the circle with radius $r$ represents the elementary particle and the circle with radius $n$ the adsorbed nitrogen molecule.

It can now be postulated that the BET surface area ($S^0{}_{\mathrm{BET}}$) of one elementary particle is given by the surface area of the sphere with radius $R$ less the surface area of the segments cut off by other elementary particles, touching the elementary particle under consideration,

$$S^0{}_{\mathrm{BET}} = 2\pi\{2(r^2 + 2rn) - a[r^2 + 2rn - r(r^2 + 2rn)^{1/2}]\} \quad (3)$$

where $a$ is the number of other touching elementary particles, which may be called the coordination number.

The volume $V_a{}^0$ of the adsorbed layer of nitrogen on one elementary particle is given by the volume of the sphere with radius $(r + t)$ less the volume of the particle with radius $r$, the volume of the segments cut off by other elementary particles and the volume of the space not accessible to nitrogen. The latter volume is given by the solid of revolution BFCGEC.

In this way the following equation (*9*) is obtained:

$$\begin{aligned} V_a{}^0 = {}& \frac{4}{3}\pi\left(3r^2t + 3rt^2 + t^3 - \frac{3art^2}{4} - \frac{at^3}{2}\right) \\ & - a\pi\left[\frac{r^3n^2(n + 2r)}{(r + n)^3} - \frac{r^2n^2(2rn + 3r^2)}{3(r + n)^3}\right. \\ & - \left\{\frac{r[n(n + 2r)]^{1/2}}{r + n} - \frac{5}{12}n\right. \\ & \left.\left.\times\left(1 - \frac{[n(n + 2r)]^{1/2}}{r + n}\right)\right\}\left(\frac{\pi n^2\theta}{360} - \frac{n^2\sin\theta}{2}\right)\right] \end{aligned} \tag{4}$$

In these equations $r$ is the radius of the elementary particle; $n$, the radius of the adsorbed molecule; $a$, the number of other elementary particles touching each elementary particle (coordination number); $t$, the actual thickness of the adsorbed layer; $\theta$, the angle formed between the radii of the adsorbed molecule, drawn through the tangent points with the elementary particles. The formal thickness $t_f$ is given by the formula

$$V_a{}^0 = t_f S^0{}_{\mathrm{BET}} \tag{5}$$

By means of Eqs. (3)–(5), the formal thickness $t_f$ can now be calculated as a function of the actual thickness $t$. The results of this calculation for the four Aerosil preparations are given in Table 1. In all calculations $n = 2.2$ Å and $a = 6.6$.

The results in Table 1 show that with the parameters used, a fairly good relationship is found between the calculated and the measured $t_f$. Only above a relative pressure of about 0.725 deviations do occur.

### *2. Influence of the Surface Curvature on the t Curve*

The treatment of the previous section leads to quite reasonable results, provided a coordination number of 6.6 is accepted. However, this number is high, as may be inferred from porosity data. The macroporosity, as calculated from the maximum bulk density of the solid after shaking, for all four samples amounts to approximately 0.97, which indicates an extremely loose packing of the agglomerates of elementary particles. More reliable information on the coordination of the elementary particles within these agglomerates, in which we are primarily interested here, may be obtained from the porosity as calculated from the density of the solid and the pore volume from nitrogen sorption data near saturation. The asymptotic behavior of the nitrogen sorption isotherm near saturation makes the definition of pore volume somewhat arbitrary, but the porosity data given in Table 2 may be considered as an indication of the order of magnitude of the porosity.

TABLE 2

Porosity of Aerosil, as Calculated from the Pore Volume

| Sample | Porosity |
|---|---|
| I | 0.88 |
| II | 0.79 |
| III | 0.79 |
| IV | 0.74 |

For a packing of spheres, the relation between porosity and coordination number has been discussed extensively by Manegold (*10*). This relation is dependent on the symmetry of the packing and for high porosity there are several possibilities for the coordination number. A coordination number of 6 would correspond to a porosity of at most 0.5, while a porosity of 0.8 points to a coordination of about 3 or even less or to an irregular packing.

If we accept a lower value for the mean coordination number of the Aerosil particles, then part of the deviations of the $t$ values for the Aerosils from the common $t$ curve has to be attributed to the influence of curvature of the surface of the solid adsorbent on the thickness of the adsorbed layer.

In Part IX (*7*) and Part XI (*11*) of this series, we have shown that in cylindrical pores and spheroidal cavities the curvature of the pore walls effects an *increase* in the thickness of the adsorbed layer, ultimately leading to complete filling of the pores and capillary condensation due to instability of the adsorbed layer. For spherical particles, an analogous effect results in a *decrease* in thickness of the adsorbed layer, as may be seen from the following argument.

Consider the transfer of $dN$ moles of vapor at pressure $p$ and temperature $T$ to the adsorbed layer of thickness $t$. If we denote the thermodynamic potential of the adsorbed layer and of the gas phase by $\mu_a(t)$ and $\mu_g$, respectively, the surface tension of the liquid–gas interface by $\gamma$, and the area of this interface by $A$, then the change in free enthalpy of the system may be written as

$$dG_{p,T} = [\mu_a(t) - \mu_g]\, dN + \gamma\, dA \qquad (6)$$

For a spherical particle $dA$ is related to $dN$ by

$$dA/dN = 2V_{\mathrm{mol}}/(r + t) \qquad (7)$$

where $V_{\mathrm{mol}}$ is the molar volume of the adsorbed phase.

As was shown in Part IX (*7*) of this series, the thermodynamic potential of the adsorbed layer may be written as $[\mu_L - F(t)]$, where $\mu_L$ is the thermodynamic potential of the bulk liquid and $F(t)$ may be evaluated from the $t$ curve of multimolecular adsorption (*1*, *2*). In equilibrium, $dG_{p,T} = 0$, so the equilibrium thickness of the adsorbed layer on a curved surface $t_e$ is related to the relative pressure by

$$RT \ln\left(\frac{p_0}{p}\right) = F(t_e) - \frac{2\gamma V_{\mathrm{mol}}}{(r + t_e)} \qquad (8)$$

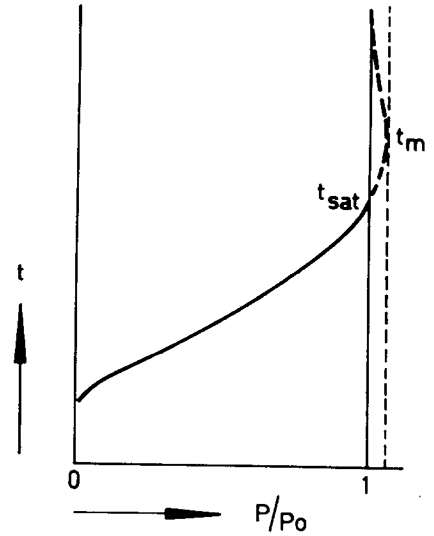

FIG. 7. Schematical representation of the adsorption on a single spherical particle.

For $p/p_0 = 1$ there is in general one finite solution for $t_e$ which we shall denote by $t_{\mathrm{sat}}$. This is also true when the form of $F(t)$ is such that on a flat surface the thickness of the adsorbed layer tends asymptotically to infinity upon approaching saturation. On the other hand, in such cases, $t = \infty$ is also a solution of (8) at saturation. Concordingly, the shape of the isotherm on a spherical particle may be sketched as represented in Fig. 7. Going from low relative pressure to saturation we reach a finite thickness of the adsorbed layer at saturation. Part of the isotherm corresponds to a metastable supersaturation branch, this equilibrium being metastable until $t_m$ is reached. The value for $t_m$ is determined by the thermodynamic stability requirement

$$d^2G/dN^2{}_{p,T} \geq 0$$

This relation also applies to the metastable branch of the isotherm but not to the unstable branch corresponding to values of $t > t_m$. Consequently, $t_m$ is given by the relation

$$-\frac{d[F(t)]}{dt} - \frac{2\gamma V_{\mathrm{mol}}}{(r + t)^2} = 0 \quad \text{for} \quad t = t_m \qquad (9)$$

In practice this supersaturation behavior will not be found for agglomerated spheres, where capillary condensation in the spheroidal cavities will take place at relative pressures below 1.

Equation (8) may be used to estimate the influence of curvature on the thickness of the adsorbed layer if we make the following simplifying assumptions:

TABLE 3

Comparison between Measured and Calculated Thickness of the Adsorbed Layer Taking into Account the Curvature of the Surface

| | | I $r = 80$ Å $S_{BET} = 162$ m²/g $a = 2.7$ $r_{corr} = 79$ Å | | | II $r = 46$ Å $S_{BET} = 281$ m²/g $a = 2.0$ $r_{corr} = 45$ Å | | | III $r = 39$ Å $S_{BET} = 333$ m²/g $a = 2.3$ $r_{corr} = 38$ Å | | | IV $r = 33$ Å $S_{BET} = 394$ m²/g $a = 3.2$ $r_{corr} = 33$ Å | | |
|---|---|---|---|---|---|---|---|---|---|---|---|---|---|
| $p/p_0$ | Common $t$ | $t_e$ | $t_f$ measured | $t_f$ calc. | $t_e$ | $t_f$ measured | $t_f$ calc. | $t_e$ | $t_f$ measured | $t_f$ calc. | $t_e$ | $t_f$ measured | $t_f$ calc. |
| 0.032 | 3 | 2.99 | 2.96 | 2.98 | 2.94 | 2.90 | 3.00 | 2.93 | 2.98 | 2.97 | 2.92 | 2.95 | 2.91 |
| 0.146 | 4 | 3.90 | 4.01 | 3.94 | 3.83 | 3.99 | 3.96 | 3.91 | 4.00 | 3.81 | 3.78 | 3.95 | 3.80 |
| 0.300 | 5 | 4.81 | 4.91 | 4.87 | 4.68 | 4.90 | 4.89 | 4.63 | 4.83 | 4.81 | 4.58 | 4.72 | 4.64 |
| 0.440 | 6 | 5.65 | 5.72 | 5.75 | 5.45 | 5.75 | 5.74 | 5.38 | 5.62 | 5.61 | 5.30 | 5.42 | 5.41 |
| 0.562 | 7 | 6.50 | 6.58 | 6.64 | 6.21 | 6.55 | 6.59 | 6.10 | 6.38 | 6.43 | 6.00 | 6.08 | 6.13 |
| 0.660 | 8 | 7.32 | 7.60 | 7.51 | 6.92 | 7.40 | 7.41 | 6.78 | 7.23 | 7.19 | 6.63 | 6.78 | 6.81 |
| 0.725 | 9 | 7.97 | 8.45 | 8.20 | 7.47 | 8.26 | 8.04 | 7.30 | 7.97 | 7.78 | 7.13 | 7.42 | 7.33 |
| 0.778 | 10 | 8.60 | 9.34 | 8.87 | 7.98 | 9.20 | 8.65 | 7.78 | 8.68 | 8.33 | 7.58 | 8.08 | 7.82 |
| 0.818 | 11 | 9.15 | 10.10 | 9.46 | 8.43 | 10.00 | 9.17 | 8.19 | 9.35 | 8.80 | 7.96 | 8.76 | 8.22 |

(a) The correction term $F(t)$ for the influence of the thickness of the adsorbed layer on the thermodynamic potential is independent of $r$, so we may use the expressions for nitrogen at its normal boiling point as given in Article X of this series (*12*).

(b) The molar volume of the adsorbate is independent of the thickness of the adsorbed layer and the curvature, and equal to that of the bulk liquid.

(c) The same applies to the surface tension of the liquid vapor interface.

These simplifications directly lead to

$$\log\left(\frac{p_0}{p}\right) = \frac{13.99}{(t_e)^2} + \frac{4.05}{(r + t_e)} - 0.034 \quad (10)$$

For each relative pressure, $t_e$ may be calculated as a function of $r$ by iteration. Using these corrected values $t_e$, we have repeated the calculations of the preceding paragraph. The coordination number $a$ in Eq. (3) and Eq. (4) is again found by trial and error to obtain the best fit to each of the experimental isotherms below $p/p_0 = 0.7$. Meanwhile, the radius $r$ compatible with (3) was calculated from $a$ and $S_{BET}$ and the calculation was again performed with this new value of $r$. This procedure was repeated until consistent values for $r$ and $a$ were obtained. The results of these calculations are presented in Table 3.

The coordination numbers thus found are all between 2 and 3, in reasonable agreement with those expected from the porosity data of Table 2. The correspondence between measured $t$ values and calculated $t$ values is quite reasonable for $p/p_0$ below 0.7. Above this relative pressure we may expect capillary condensation in the cavities in between the particles to become important and eventually to take over. In order to decide between the two possibilities discussed in the present paper it would be worthwhile to obtain independent information on the packing and coordination number of elementary particles in Aerosil, but this information is not available at the moment.

## References

*1.* de Boer, J. H., Linsen, B. G., and Osinga, Th. J., *J. Catalysis* **4**, 643 (1965).

*2.* Lippens, B. C., Linsen, B. G., and de Boer, J. H., *J. Catalysis* **3**, 32 (1964).

*3.* Brunauer, S., Emmett, P. H., and Teller, E., *J. Am. Chem. Soc.* **60**, 309 (1938).

*4.* de Boer, J. H., Broekhoff, J. C. P., Linsen, B. G., and Meijer, A. L., *J. Catalysis* **7**, 135 (1967).

*5.* Geus, J. W., and Kiel, A. M., Communicated at the Meeting of the Dutch Society of Electron Microscopy, Utrecht, The Netherlands, 1966.

*6.* Okkerse, C., Thesis, Technological University of Delft, The Netherlands, 1961.

*7.* Broekhoff, J. C. P., and de Boer, J. H., *J. Catalysis* **9**, 8 (1967).

*8.* Wagner, E., and Brünner, H., *Angew. Chem.* **72**, 744 (1960).

*9.* Linsen, B. G., Thesis, Technological University of Delft, The Netherlands, 1964.

*10.* Manegold, E., "Kapillarsysteme," p. 245. Chemie und Technik, Verlaggesellschaft, Heidelberg, Germany, 1955.

*11.* Broekhoff, J. C. P., and de Boer, J. H., *J. Catalysis* **10,** 153 (1968).

*12.* Broekhoff, J. C. P., and de Boer, J. H., *J. Catalysis* **9,** 15 (1967).